NEURORADIOLOGY

I J Radiol. 2024 July; 21(3): e153698 https://doi.org/10.5812/iranjradiol-153698

Published Online: 2024 July 30

Research Article

Quantifying Iron Accumulation in Deep Gray Matter Nuclei of Patients with Mild Traumatic Brain Injury Using Quantitative Susceptibility Mapping: A Comparative Study with Healthy Controls

Abolfazl Mahmoudi [1], Hassan Goodarzi [2], Bahman Jalali Kondori [1,2], Ramezan Jafari [3], Mehdi Raei [4], Mostafa Eslamimahmoudabadi [5], Ali Reza Eftekhari Moqadam [1,*]

[1] Department of Anatomical Science, Faculty of Medicine, Baqiyatallah University of Medical Sciences, Tehran, Iran
[2] Baqiyatallah Research Center for Gastroenterology and Liver Diseases (BRCGL), Baqiyatallah University of Medical Sciences, Tehran, Iran
[3] Chemical Injuries Research Center, Baqiyatallah University of Medical Sciences, Tehran, Iran
[4] Health Research Center, Life Style Institute, Baqiyatallah University of Medical Sciences, Tehran, Iran
[5] Student Research Committee, Baqiyatallah University of Medical Sciences, Tehran, Iran

[*] ***Corresponding Author:*** Department of Anatomical Science, Faculty of Medicine, Baqiyatallah University of Medical Sciences, Tehran, Iran. Email: eftekhari.ar@ajums.ac.ir

Received: 30 January, 2024; **Revised:** 23 June, 2024; **Accepted:** 21 July, 2024

Abstract

Background: Mild traumatic brain injury (mTBI) is a common neurological condition characterized by subtle brain dysfunction. Although generally considered less severe than moderate and severe TBI, it can have significant consequences on cognitive and motor function. Iron deposition in the basal ganglia nuclei, particularly in individuals with mTBI, has been reported as a potential biomarker for neurodegenerative and neurocognitive changes following injury. While previous studies have explored the relationship between iron deposition and mTBI, few human studies have examined these changes using quantitative susceptibility mapping (QSM). The QSM is a powerful technique that enables the non-invasive measurement of iron content in deep brain structures, providing valuable insights into the pathophysiology of mTBI.

Objectives: This study aimed to compare magnetic susceptibility values (iron content) in the deep gray matter (DGM) nuclei regions of patients with mTBI and healthy controls (HCs).

Patients and Methods: In this case-control study, we enrolled 10 acute mTBI patients and 10 age-matched HCs who underwent imaging with a 3 Tesla Prisma scanner magnetic resonance imaging (MRI), including T1 weighted magnetization-prepared rapid gradient echo (T1-MPRAGE) and multi-echo 3D gradient-recalled echo (GRE) sequences for QSM reconstruction. Inclusion criteria included patients aged 16 - 50 years, a Glasgow Coma Scale (GCS) score of 13 - 15 upon emergency department arrival, and a history of loss of consciousness for less than 30 minutes. Exclusion criteria included prior brain injuries, neurological disorders, psychiatric conditions, or substance abuse. The magnetic susceptibility of the DGM nuclei was calculated using the streaking artifact reduction for QSM (STAR-QSM) technique. Group comparisons were performed using independent *t*-tests.

Results: Significantly higher magnetic susceptibility values were observed in the DGM nuclei regions, specifically in the right caudate ($P < 0.001$), left caudate ($P = 0.002$), right thalamus ($P = 0.004$), and right hippocampus ($P = 0.002$), in mTBI patients compared to HCs.

Conclusion: These findings suggest that mTBI may be associated with alterations in iron content or magnetic susceptibility within the DGM nuclei regions compared to HCs, potentially reflecting microstructural changes. This study provides preliminary evidence for the potential of QSM as a tool for investigating tissue susceptibility in acute mTBI. Future research should focus on longitudinal studies with larger sample sizes to examine the temporal evolution of iron accumulation and its potential relationship with functional outcomes in mTBI patients.

Keywords: Mild Traumatic Brain Injury, MRI, Quantitative Susceptibility Mapping, Deep Grey Matter Nuclei, Iron Accumulation

1. Background

Mild traumatic brain injury (mTBI), commonly known as concussion, is a prevalent condition, accounting for 70 - 90% of all treated brain injuries, with an incidence rate of approximately 100 - 300 cases per 100,000 people (1, 2). Despite being classified as "mild", mTBI can lead to various complications and long-term consequences, including neuropathological and neurocognitive changes (3, 4). Studies have demonstrated a correlation between iron accumulation and cognitive dysfunction in patients with chronic mTBI (5, 6). Longitudinal studies are ongoing to better understand the cascade of events that lead to iron accumulation in the brain following acute mTBI (7).

Accumulating evidence suggests that iron dysregulation and deposition play a crucial role in the pathogenesis of mTBI, contributing to oxidative stress, excitotoxicity, and cell injury, as well as disruption of the blood-brain barrier and subsequent neuronal damage (8). Iron is a micronutrient essential for various cellular functions, including energy metabolism, nucleic acid synthesis, and cell proliferation (9). However, excessive iron levels can generate reactive oxygen species (ROS),

which can damage cellular components such as lipids, proteins, and DNA (10, 11). This oxidative damage occurs because excess iron catalyzes the formation of hydroxyl radicals through reactions with hydrogen peroxide, a process known as Fenton's chemistry (11). Additionally, ROS mediate ferroptosis, a newly recognized form of non-apoptotic cell death that occurs after TBI (12, 13). Studies have shown that iron accumulation in the brain, particularly in deep gray matter (DGM) regions, may contribute to the pathophysiology of mTBI-related cognitive impairments and post-traumatic headache, potentially serving as a biomarker for these conditions (14-16).

Advanced imaging techniques have played a crucial role in elucidating the role of iron in the pathophysiology of mTBI (17). These imaging modalities provide valuable insights into the distribution and impact of iron in the post-mTBI brain, aiding in the identification of potential therapeutic targets. Magnetic resonance imaging (MRI) is a powerful tool for diagnosing various medical conditions. Susceptibility-weighted imaging (SWI) is an MRI technique that visualizes tissues with high magnetic susceptibility by combining magnitude and phase information to display variations in the tissue magnetic field (18). However, SWI is affected by regional field effects and image artifacts, which are influenced by imaging parameters (19-21). Although SWI has been used for diagnosing and monitoring conditions involving iron deposition, such as neurodegenerative diseases and neuromuscular disorders (22-24), its diagnostic performance is lower than that of quantitative susceptibility mapping (QSM). Additionally, SWI provides only qualitative information regarding tissue magnetic susceptibility (25, 26).

The QSM is a post-processing technique that quantifies iron distribution in the brain and is superior to other techniques such as T2* and SWI (27). The QSM measures magnetic susceptibility using MRI phase and magnitude data. The relationship between magnetic susceptibility, as assessed by QSM, and iron accumulation in brain tissues has been previously reported (28). The QSM enables accurate mapping of iron deposition in various neurological conditions (29). The ability of QSM to precisely map iron deposition and other pathophysiological changes makes it a valuable tool for understanding mTBI and its associated complications, paving the way for improved diagnostic and management strategies.

2. Objectives

This study hypothesizes that mTBI is associated with increased iron deposition in the DGM nuclei, which can be measured using QSM, thereby providing new insights into mTBI pathophysiology.

Although previous studies have investigated changes in iron levels and magnetic susceptibility in different brain regions in both patients and animal models, few studies have examined iron alterations in mTBI patients using the QSM technique. The present study aimed to assess changes in magnetic susceptibility values in the DGM nuclei of individuals with mTBI using QSM.

3. Patients and Methods

3.1. Ethics Statement

The Research Ethics Committee of Baqiyatallah Hospital approved this study (ethical code: IR.BMSU.BAQ.REC.1402.032). All participants with potentially identifiable images or data provided written informed consent before inclusion in the study. Additionally, patients and healthcare providers were briefed on the study details and provided informed written consent before data collection.

3.2. Participants

The criteria for including mild TBI patients were based on the World Health Organization's Collaborating Center for Neuro-Trauma Task Force guidelines (30). Patients were involved in motor vehicle accidents (MVA) or were pedestrians with confirmed head trauma and a Glasgow Coma Scale (GCS) score of 13 - 15 upon arrival at the emergency department of Baqiyatallah Hospital. They exhibited specific symptoms such as loss of consciousness for less than 30 minutes and post-traumatic amnesia (PTA) for less than 24 hours. Magnetic resonance imaging imaging was conducted within 14 days of injury. Eligible patients were between 16 and 45 years old. To minimize the effect of age on iron deposition results, only individuals under 45 years old were included.

Exclusion criteria included a history of previous brain injuries, neurological diseases, psychiatric conditions, substance abuse, structural brain abnormalities, skull fractures, sedative use, and penetrating craniocerebral injuries.

In this study, we selected ten patients (age range: 25 - 45 years) with mTBI who presented to the National Brain Mapping Laboratory (NBML, Tehran, Iran) and were approximately 14 days post-injury at the time of MRI imaging. Additionally, we selected ten healthy subjects through purposive sampling. Participants were chosen

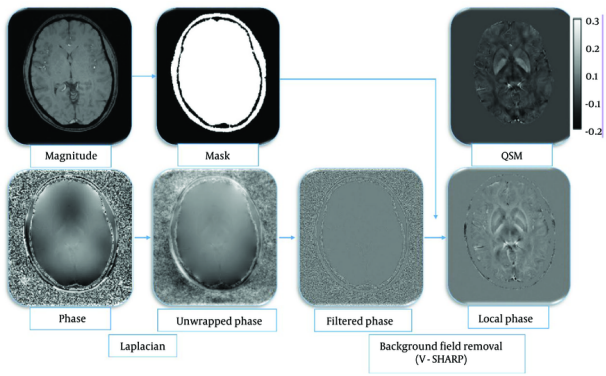

Figure 1. Illustration of the reconstruction process of the quantitative susceptibility mapping (QSM) imaging technique: Magnitude QSM imaging technique. Magnitude images were used for mask creation; magnitude images were utilized for mask creation. The phase images were first processed using the Laplacian unwrapping method, and then the filtered phase images were obtained. The local phase was obtained using the variable-kernel sophisticated harmonic artifact reduction for phase data (V-SHARP) method, and ultimately, susceptibility maps were achieved using the streaking artifact reduction for QSM (STAR-QSM) method.

based on inclusion (age, sex, handedness) and exclusion (history of trauma and psychiatric disorders) criteria. The healthy controls (HCs) were carefully matched to the mTBI patients in terms of age, sex, and handedness.

3.3. Magnetic Resonance Imaging Protocol

Magnetic resonance imaging images were acquired using a 3.0 Tesla scanner (Prisma, Siemens, Erlangen, München, Germany) equipped with a superconductive zero-helium boil-off 3T magnet at the NBML center and a 20-channel head and neck coil. A 3D T1-weighted magnetization-prepared rapid gradient echo (T1-MPRAGE) sequence was used to obtain high-resolution structural MRI data, consisting of 176 slices with no gap and a voxel resolution of $1 \times 1 \times 1$ mm (TR = 1800 ms, TE = 2 ms, scan time = 4 min, voxel resolution = $1 \times 1 \times 1$ mm, slice thickness = 1 mm, field of view (FOV) read = 255 mm, FOV phase = 100%).

Susceptibility-weighted imaging was performed using a 3D gradient-recalled echo (GRE) sequence with the following parameters: TR = 30 ms, TE1 = 6 ms, number of echoes = 5, flip angle = 15°, voxel resolution = $0.8 \times 0.8 \times 2$ mm, and slices per slab = 72.

3.4. Quantitative Susceptibility Mapping Analysis

The QSM was reconstructed from SWI sequence data acquisition through a series of steps outlined in methodological studies: Phase unwrapping using the Laplacian-based method (31), background field removal employing the variable-kernel sophisticated harmonic artifact reduction for phase data (V-SHARP) method (32-34), and field-to-susceptibility inversion using the streaking artifact reduction for QSM (STAR-QSM) method (35) (Figure 1).

The QSM calculations were conducted using MATLAB 2022b (MathWorks, Natick, MA) and the STI Suite, a MATLAB toolbox version 3.0 package (31). The resulting QSM images were analyzed to assess tissue magnetic susceptibility properties, including the presence of iron accumulation in the DGM nuclei.

Before segmentation, the QSM images were registered onto T1-weighted images using SPM 12 software. The T1-weighted images were then used for segmenting the DGM nuclei, including the thalamus, caudate nucleus, globus pallidus, putamen, amygdala, and hippocampus, using FSL software. The extracted masks were applied for the segmentation of the QSM images. Segmentation was performed to calculate magnetic susceptibility indices in the targeted regions.

3.5. Statistical Analyses

Assumptions of normality were assessed using the Shapiro-Wilk test. The significance level was set at $\alpha = 0.05$. Group differences were analyzed using independent *t*-tests for normally distributed data and Mann-Whitney U tests for non-normally distributed data. To control for Type I error due to multiple comparisons across the 12 brain regions, a Bonferroni correction was applied, adjusting the significance threshold to $P < 0.0041$ (0.05/12). All statistical analyses were performed using SPSS 16 (SPSS Inc. Released 2007. SPSS for Windows, Version 16.0. Chicago, SPSS Inc.).

Table 1. Characteristics of the Participants Enrolled in the Study, Including Patients with Mild Traumatic Brain Injury and Healthy Controls [a]

Variables	mTBI (N = 10)	HC (N = 10)	P-value [b]
Sex (male)	6 (60)	6 (60)	1.000
Age (y)	34.2 ± 10.8	31.6 ± 13.4	0.63
Handedness (right)	10 (100)	10 (100)	1.000
DAI	-	-	-

Abbreviations: mTBI, mild traumatic brain injury; HC, healthy control.

[a] Values are expressed as No. (%) or mean ± SD.

[b] $P < 0.05$ considered significant.

Table 2. Shapiro-Wilk Test Results for Assessment of Normality of the Variables

	Shapiro-Wilk test		
Region	**Statistic**	**df**	**P-value**
R_putamen	0.514	20	0.000
L_putamen	0.948	20	0.341
R_caudate	0.855	20	007
L_caudate	0.765	20	0.000
R_thalamus	0.796	20	0.001
L_thalamus	0.624	20	0.000
R_ globus pallidus	0.700	20	0.000
L_ globus pallidus	0.770	20	0.000
R_amygdala	0.800	20	0.001
L_amygdala	0.874	20	0.014
R_hippocumpus	0.737	20	0.000
L_hippocampus	0.785	20	0.001

4. Results

We collected data from 10 mTBI patients and 10 HCs. No significant differences were found between the mTBI and HC groups in terms of age, sex, or handedness (all participants were right-handed) (Table 1).

The results of the Shapiro-Wilk test indicated that, except for the left putamen variable, all other variables were not normally distributed (Table 2). The mean, standard deviation, mean difference, 95% confidence interval for the mean difference as an effect size, and P-value for comparing means between the two groups (mTBI patients and HCs) are presented in Table 3.

Significant differences in magnetic susceptibility were observed in the right caudate ($P < 0.001$), left caudate ($P = 0.002$), right thalamus ($P = 0.004$), and right hippocampus ($P = 0.002$) (Table 3 and Figure 2). The results for other regions, including the right putamen ($P = 0.06$), left putamen ($P = 0.02$), left thalamus ($P = 0.005$), right globus pallidus ($P = 0.007$), left globus pallidus ($P = 0.007$), right amygdala ($P = 0.06$), left amygdala ($P = 0.02$), and left hippocampus ($P = 0.02$), were not statistically significant.

The mean, standard deviation, mean difference and 95% confidence interval for mean difference as effect size and P-value for comparing means in two groups of patients and HCs. The significance level was $P < 0.0041$ (0.05/12).

5. Discussion

This study aimed to evaluate alterations in iron deposition (magnetic susceptibility) in the basal ganglia and thalamus of mTBI patients using the QSM technique. While white matter is also important in the context of brain injury, our primary focus on DGM was driven by the well-established involvement of these regions in cognitive and neurological impairments associated with mTBI.

Our findings revealed a notable increase in magnetic susceptibility values within the DGM nuclei regions in an average of ten patients. These changes were significant in the right and left caudate nuclei, right

Table 3. Comparison of Mean Magnetic Susceptibility of the Subcortical Brain Nuclei Between the Mild Traumatic Brain Injury and Healthy Controls

Variables and groups	Mean ± SD	Mean difference	95% Confidence interval of the difference		P-value
			Lower bound	Upper bound	
R_putamen		0.002	-0.0011	0.0069	0.06
Patient	0.023 ± 0.006				
Control	0.020 ± 0.0008				
L_putamen		0.001	0.0001	0.0022	0.02
Patient	0.020 ± 0.001				
Control	0.019 ± 0.0009				
R_caudate		0.004	0.0016	0.0068	< 0.001
Patient	0.029 ± 0.003				
Control	0.025 ± 0.001				
L_caudate		0.005	0.0016	0.0083	0.002
Patient	0.030 ± 0.005				
Control	0.025 ± 0.0008				
R_thalamus		0.0009	0.0003	0.0015	0.004
Patient	0.002 ± 0.0008				
Control	0.001 ± 0.0001				
L_thalamus		0.0009	0.00009	0.0018	0.05
Patient	0.002 ± 0.001				
Control	0.001 ± 0.0001				
R_ globus pallidus		0.016	0.0042	0.0280	0.007
Patient	0.046 ± 0.01				
Control	0.030 ± 0.001				
L_ globus pallidus		0.012	0.0040	0.0212	0.007
Patient	0.043 ± 0.01				
Control	0.031 ± 0.001				
R_amygdala		0.001	0.0003	0.0030	0.06
Patient	0.006 ± 0.002				
Control	0.004 ± 0.0004				
L_amygdala		0.001	0.0005	0.0026	0.02
Patient	0.006 ± 0.001				
Control	0.005 ± 0.0005				
R_hippocumpus		0.001	0.0004	0.0025	0.002
Patient	0.003 ± 0.001				
Control	0.002 ± 0.0003				
L_hippocampus		0.001	0.0003	0.0020	0.02
Patient	0.003 ± 0.001				
Control	0.002 ± 0.0002				

thalamus, and right hippocampus. These results suggest a potential link between mTBI and iron deposition in the brain, contributing to our understanding of the role of iron accumulation in mTBI pathophysiology.

The DGM nuclei house critical structures, such as the basal ganglia and thalamus, which play a vital role in motor control, cognition, executive functions, and emotional regulation (36). Higher iron deposition in the thalamus and hypothalamus has been correlated with poor memory performance, while higher iron levels in the caudate nucleus have been linked to cognitive decline (37). Iron is essential for various neurological functions, but excess iron can lead to oxidative stress and neurotoxicity (38), potentially contributing to mTBI symptoms such as fatigue, cognitive decline, and movement disorders (14, 15).

To understand the long-term pathogenesis resulting from TBI, Onyszchuk et al. subjected mice to controlled impact and performed MRI scans on their brains two months post-injury. The results revealed a decrease in T2 signal in the injured side of the thalamus, indicating increased iron levels in this region (39). The initial study

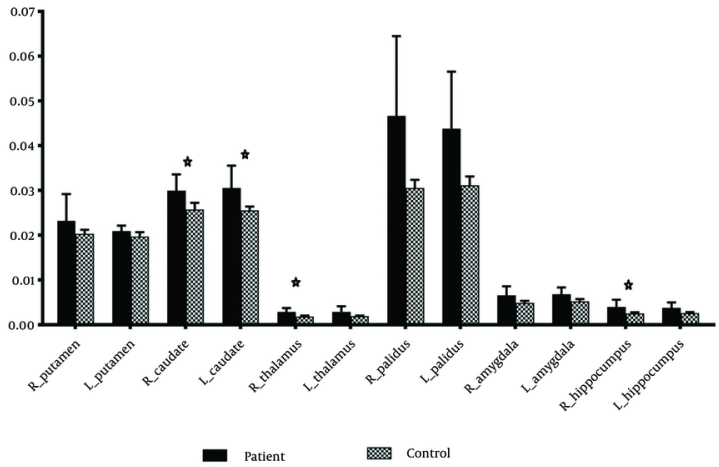

Figure 2. Magnetic susceptibility values in healthy subjects and mild traumatic brain injury (mTBI) patients. * indicates significance between the different areas.

examining iron accumulation in the DGM nuclei included 28 patients with mTBI. The results showed a significant increase in magnetic field correlation values within the thalamus and globus pallidus of mTBI patients, indicating iron accumulation. These findings support the idea that DGM nuclei are affected by mTBI and suggest a potential association between iron accumulation and pathophysiological processes following mTBI (7).

To confirm these post-injury changes, Liu et al. collected brain tissue samples from 19 patients undergoing surgical intervention for TBI 3 - 17 days after trauma. Tissue iron deposition and ferritin heavy chain expression were measured using tissue staining, polymerase chain reaction, western blot, and immunohistochemistry, showing an increase in ferritin chain expression and iron accumulation in the brain (40). In a study conducted six months post-injury using SWI phase images, an increase in the radian angle was observed in various brain regions, such as the thalamus, lenticular nucleus, hippocampus, substantia nigra, and red nucleus (5).

Several studies have also investigated changes in iron levels in the brain following injury using the QSM technique. Among these, Lin et al. reported changes in the thalamus 14 days after mTBI (41). Additionally, a recent study by Koch et al. on athletes two days after mTBI reported a general decrease in magnetic susceptibility values in the DGM regions (42). In contrast, some studies have indicated no significant changes in magnetic susceptibility values in the DGM regions of individuals with brain injury (43, 44).

An increase in magnetic susceptibility values in the DGM nuclei likely indicates iron deposition resulting from neuroinflammatory processes following mTBI. Trauma-induced disruption of the blood-brain barrier may facilitate iron accumulation in brain tissue, accompanied by oxidative stress and neuronal damage. This process creates a vicious cycle, where the generation of ROS and subsequent activation of microglia further contribute to iron dysregulation. Over time, these pathophysiological changes may lead to cell death, resulting in the long-term cognitive and motor impairments commonly observed in mTBI patients. Understanding these mechanisms in detail is crucial, as identifying them could lay the foundation for potential therapeutic interventions, such as iron chelation therapy, which may mitigate the effects of mTBI.

Our study had several limitations. The relatively small sample size necessitates further research to confirm these findings. Financial and time constraints, as well as limited access to participants, contributed to the small sample size. However, given this limitation, researchers prioritized data quality and measurement accuracy. Despite the small sample size, a significant difference was observed between the two groups. Nonetheless, it is important to acknowledge the impact of the limited sample size on the study's ability to draw strong conclusions and its implications for the generalizability of the findings. The sample size was determined based on feasibility and the exploratory

nature of the study. Additionally, longitudinal studies with larger cohorts are needed to track iron accumulation patterns over time and understand their association with mTBI recovery.

Further investigation is required to determine the precise timeline of iron accumulation following mTBI and its potential correlation with symptom severity and long-term outcomes. Additionally, exploring iron chelation therapy as a potential intervention for mTBI patients with iron overload is warranted.

In conclusion, our findings revealed iron deposition in the DGM nuclei of mTBI patients. These regions are integral components of cognitive networks, suggesting that alterations in iron levels may disrupt these circuits and contribute to the diverse clinical manifestations of mTBI, including neuropathological, neurophysiological, and neurocognitive changes. While replication in larger cohorts and longitudinal studies is necessary, these findings underscore the potential of quantitative neuroimaging biomarkers, such as QSM, to non-invasively characterize neural pathology involving iron in mTBI. Future research should further explore the role of iron in mTBI pathophysiology and investigate the potential for iron-targeted therapies to improve patient outcomes.

Footnotes

Authors' Contribution: Study concept and design: A. E., H. G., and R. J.; Acquisition of data: A. M. and M. E.; Analysis and interpretation of data: A. M. and M. R.; Drafting of the manuscript: A. M.; Critical revision of the manuscript for important intellectual content: B. J. and A. E.; Statistical analysis: M. R. and A. M.

Conflict of Interests Statement: The authors declare that they have no conflicts of interest.

Data Availability: The dataset presented in the study is available on request from the corresponding author during submission or after publication.

Ethical Approval: IR.BMSU.BAQ.REC.1402.032 .

Funding/Support: This research received no external funding; thanks to guidance and advice from "Clinical Research Development Unit of Baqiyatallah Hospital".

Informed Consent: All participants with potentially identifiable images or data provided written informed consent before inclusion in the study.

References

1. Cassidy JD, Carroll LJ, Peloso PM, Borg J, von Holst H, Holm L, et al. Incidence, risk factors and prevention of mild traumatic brain injury: results of the WHO Collaborating Centre Task Force on Mild Traumatic Brain Injury. *J Rehabil Med*. 2004;(43 Suppl):28-60. [PubMed ID: 15083870]. https://doi.org/10.1080/16501960410023732.
2. Carroll LJ, Cassidy J, Peloso PM, Borg J, von Holst H, Holm L, et al. Prognosis for mild traumatic brain injury: results of the WHO Collaborating Centre Task Force on Mild Traumatic Brain Injury. *J Rehabil Med*. 2004;(43 Suppl):84-105. [PubMed ID: 15083873]. https://doi.org/10.1080/16501960410023859.
3. Ryan LM, Warden DL. Post concussion syndrome. *Int Rev Psychiat*. 2003;**15**(4):310-6. [PubMed ID: 15276952]. https://doi.org/10.1080/09540260310001606692.
4. Ahman S, Saveman BI, Styrke J, Bjornstig U, Stalnacke BM. Long-term follow-up of patients with mild traumatic brain injury: a mixed-method study. *J Rehabil Med*. 2013;**45**(8):758-64. [PubMed ID: 24002311]. https://doi.org/10.2340/16501977-1182.
5. Lu L, Cao H, Wei X, Li Y, Li W. Iron Deposition Is Positively Related to Cognitive Impairment in Patients with Chronic Mild Traumatic Brain Injury: Assessment with Susceptibility Weighted Imaging. *Biomed Res Int*. 2015;**2015**:470676. [PubMed ID: 26798636]. [PubMed Central ID: PMC4698517]. https://doi.org/10.1155/2015/470676.
6. Huang S, Li S, Feng H, Chen Y. Iron Metabolism Disorders for Cognitive Dysfunction After Mild Traumatic Brain Injury. *Front Neurosci*. 2021;**15**:587197. [PubMed ID: 33796002]. [PubMed Central ID: PMC8007909]. https://doi.org/10.3389/fnins.2021.587197.
7. Raz E, Jensen JH, Ge Y, Babb JS, Miles L, Reaume J, et al. Brain iron quantification in mild traumatic brain injury: a magnetic field correlation study. *AJNR Am J Neuroradiol*. 2011;**32**(10):1851-6. [PubMed ID: 21885717]. [PubMed Central ID: PMC3848044]. https://doi.org/10.3174/ajnr.A2637.
8. Sun A, Blecharz-Lang KG, Małecki A, Meybohm P, Nowacka-Chmielewska MM, Burek M. Role of microRNAs in the regulation of blood-brain barrier function in ischemic stroke and under hypoxic conditions in vitro. *Front Drug Deliv*. 2022;**2**. https://doi.org/10.3389/fddev.2022.1027098.
9. Moreira AC, Mesquita G, Gomes MS. Ferritin: An Inflammatory Player Keeping Iron at the Core of Pathogen-Host Interactions. *Microorganisms*. 2020;**8**(4). [PubMed ID: 32325688]. [PubMed Central ID: PMC7232436]. https://doi.org/10.3390/microorganisms8040589.
10. Ying JF, Lu ZB, Fu LQ, Tong Y, Wang Z, Li WF, et al. The role of iron homeostasis and iron-mediated ROS in cancer. *Am J Cancer Res*. 2021;**11**(5):1895-912. [PubMed ID: 34094660]. [PubMed Central ID: PMC8167679].
11. Iwasaki K, Hailemariam K, Tsuji Y. PIAS3 interacts with ATF1 and regulates the human ferritin H gene through an antioxidant-responsive element. *J Biol Chem*. 2007;**282**(31):22335-43. [PubMed ID: 17565989]. [PubMed Central ID: PMC2409283]. https://doi.org/10.1074/jbc.M701477200.
12. Kenny EM, Fidan E, Yang Q, Anthonymuthu TS, New LA, Meyer EA, et al. Ferroptosis Contributes to Neuronal Death and Functional Outcome After Traumatic Brain Injury. *Crit Care Med*. 2019;**47**(3):410-8. [PubMed ID: 30531185]. [PubMed Central ID: PMC6449247]. https://doi.org/10.1097/CCM.0000000000003555.
13. Tang S, Gao P, Chen H, Zhou X, Ou Y, He Y. The Role of Iron, Its Metabolism and Ferroptosis in Traumatic Brain Injury. *Front Cell Neurosci*. 2020;**14**:590789. [PubMed ID: 33100976]. [PubMed Central ID: PMC7545318]. https://doi.org/10.3389/fncel.2020.590789.
14. Nikolova S, Schwedt TJ, Li J, Wu T, Dumkrieger GM, Ross KB, et al. T2* reduction in patients with acute post-traumatic headache. *Cephalalgia*. 2022;**42**(4-5):357-65. [PubMed ID: 34644192]. https://doi.org/10.1177/03331024211048509.

15. Chong CD, Nikolova S, Dumkrieger G, Wu T, Berisha V, Li J, et al. Thalamic subfield iron accumulation after acute mild traumatic brain injury as a marker of future post-traumatic headache intensity. *Headache*. 2023;**63**(1):156-64. [PubMed ID: 36651577]. [PubMed Central ID: PMC10184776]. https://doi.org/10.1111/head.14446.
16. Mahmoudi Aqeel-Abadi A, Fateh HR, Masoudnia S, Shirzad N, Seyfi M, Ebrahimi T, et al. A Preliminary Study of Alterations in Iron Disposal and Neural Activity in Ischemic Stroke. *Biomed Res Int*. 2022;**2022**:4552568. [PubMed ID: 35971446]. [PubMed Central ID: PMC9375706]. https://doi.org/10.1155/2022/4552568.
17. Nisenbaum EJ, Novikov DS, Lui YW. The presence and role of iron in mild traumatic brain injury: an imaging perspective. *J Neurotrauma*. 2014;**31**(4):301-7. [PubMed ID: 24295521]. [PubMed Central ID: PMC3922137]. https://doi.org/10.1089/neu.2013.3102.
18. Liu MY, Chen ZY, Li JF, Xiao HF, Ma L. Quantitative susceptibility-weighted imaging in amyotrophic lateral sclerosis with 3.0 T magnetic resonance imaging. *J Int Med Res*. 2021;**49**(2):300060521992222. [PubMed ID: 33583226]. [PubMed Central ID: PMC7890729]. https://doi.org/10.1177/0300060521992222.
19. Haacke EM, Mittal S, Wu Z, Neelavalli J, Cheng YC. Susceptibility-weighted imaging: technical aspects and clinical applications, part 1. *AJNR Am J Neuroradiol*. 2009;**30**(1):19-30. [PubMed ID: 19039041]. [PubMed Central ID: PMC3805391]. https://doi.org/10.3174/ajnr.A1400.
20. Mittal S, Wu Z, Neelavalli J, Haacke EM. Susceptibility-weighted imaging: technical aspects and clinical applications, part 2. *AJNR Am J Neuroradiol*. 2009;**30**(2):232-52. [PubMed ID: 19131406]. [PubMed Central ID: PMC3805373]. https://doi.org/10.3174/ajnr.A1461.
21. Haller S, Haacke EM, Thurnher MM, Barkhof F. Susceptibility-weighted Imaging: Technical Essentials and Clinical Neurologic Applications. *Radiology*. 2021;**299**(1):3-26. [PubMed ID: 33620291]. https://doi.org/10.1148/radiol.2021203071.
22. Schweitzer AD, Liu T, Gupta A, Zheng K, Seedial S, Shtilbans A, et al. Quantitative susceptibility mapping of the motor cortex in amyotrophic lateral sclerosis and primary lateral sclerosis. *AJR Am J Roentgenol*. 2015;**204**(5):1086-92. [PubMed ID: 25905946]. [PubMed Central ID: PMC4889122]. https://doi.org/10.2214/AJR.14.13459.
23. Lee JY, Lee YJ, Park DW, Nam Y, Kim SH, Park J, et al. Quantitative susceptibility mapping of the motor cortex: a comparison of susceptibility among patients with amyotrophic lateral sclerosis, cerebrovascular disease, and healthy controls. *Neuroradiology*. 2017;**59**(12):1213-22. [PubMed ID: 29018934]. https://doi.org/10.1007/s00234-017-1933-9.
24. Welton T, Maller JJ, Lebel RM, Tan ET, Rowe DB, Grieve SM. Diffusion kurtosis and quantitative susceptibility mapping MRI are sensitive to structural abnormalities in amyotrophic lateral sclerosis. *Neuroimage Clin*. 2019;**24**:101953. [PubMed ID: 31357149]. [PubMed Central ID: PMC6664242]. https://doi.org/10.1016/j.nicl.2019.101953.
25. Liu C, Li W, Tong KA, Yeom KW, Kuzminski S. Susceptibility-weighted imaging and quantitative susceptibility mapping in the brain. *J Magn Reson Imaging*. 2015;**42**(1):23-41. [PubMed ID: 25270052]. [PubMed Central ID: PMC4406874]. https://doi.org/10.1002/jmri.24768.
26. Adams LC, Bressem K, Boker SM, Bender YY, Norenberg D, Hamm B, et al. Diagnostic performance of susceptibility-weighted magnetic resonance imaging for the detection of calcifications: A systematic review and meta-analysis. *Sci Rep*. 2017;**7**(1):15506. [PubMed ID: 29138506]. [PubMed Central ID: PMC5686169]. https://doi.org/10.1038/s41598-017-15860-1.
27. Shmueli K, de Zwart JA, van Gelderen P, Li TQ, Dodd SJ, Duyn JH. Magnetic susceptibility mapping of brain tissue in vivo using MRI phase data. *Magn Reson Med*. 2009;**62**(6):1510-22. [PubMed ID: 19859937]. [PubMed Central ID: PMC4275127]. https://doi.org/10.1002/mrm.22135.
28. Langkammer C, Schweser F, Krebs N, Deistung A, Goessler W, Scheurer E, et al. Quantitative susceptibility mapping (QSM) as a means to measure brain iron? A post mortem validation study. *Neuroimage*. 2012;**62**(3):1593-9. [PubMed ID: 22634862]. [PubMed Central ID: PMC3413885]. https://doi.org/10.1016/j.neuroimage.2012.05.049.
29. Wang Y, Liu T. Quantitative susceptibility mapping (QSM): Decoding MRI data for a tissue magnetic biomarker. *Magn Reson Med*. 2015;**73**(1):82-101. [PubMed ID: 25044035]. [PubMed Central ID: PMC4297605]. https://doi.org/10.1002/mrm.25358.
30. Borg J, Holm L, Cassidy JD, Peloso PM, Carroll LJ, von Holst H, et al. Diagnostic procedures in mild traumatic brain injury: results of the WHO Collaborating Centre Task Force on Mild Traumatic Brain Injury. *J Rehabil Med*. 2004;(43 Suppl):61-75. [PubMed ID: 15083871]. https://doi.org/10.1080/16501960410023822.
31. Li W, Avram AV, Wu B, Xiao X, Liu C. Integrated Laplacian-based phase unwrapping and background phase removal for quantitative susceptibility mapping. *NMR Biomed*. 2014;**27**(2):219-27. [PubMed ID: 24357120]. [PubMed Central ID: PMC3947438]. https://doi.org/10.1002/nbm.3056.
32. Fang J, Bao L, Li X, van Zijl PCM, Chen Z. Background field removal using a region adaptive kernel for quantitative susceptibility mapping of human brain. *J Magn Reson*. 2017;**281**:130-40. [PubMed ID: 28595120]. [PubMed Central ID: PMC5846686]. https://doi.org/10.1016/j.jmr.2017.05.004.
33. Kan H, Arai N, Takizawa M, Omori K, Kasai H, Kunitomo H, et al. Background field removal technique based on non-regularized variable kernels sophisticated harmonic artifact reduction for phase data for quantitative susceptibility mapping. *Magn Reson Imaging*. 2018;**52**:94-101. [PubMed ID: 29902566]. https://doi.org/10.1016/j.mri.2018.06.006.
34. Wang C, Foxley S, Ansorge O, Bangerter-Christensen S, Chiew M, Leonte A, et al. Methods for quantitative susceptibility and R2* mapping in whole post-mortem brains at 7T applied to amyotrophic lateral sclerosis. *Neuroimage*. 2020;**222**:117216. [PubMed ID: 32745677]. [PubMed Central ID: PMC7775972]. https://doi.org/10.1016/j.neuroimage.2020.117216.
35. Wei H, Dibb R, Zhou Y, Sun Y, Xu J, Wang N, et al. Streaking artifact reduction for quantitative susceptibility mapping of sources with large dynamic range. *NMR Biomed*. 2015;**28**(10):1294-303. [PubMed ID: 26313885]. [PubMed Central ID: PMC4572914]. https://doi.org/10.1002/nbm.3383.
36. Mercadante AA, Tadi P. *Neuroanatomy, gray matter*. Treasure Island: StatPearls Publishing; 2020.
37. Spence H, McNeil CJ, Waiter GD. The impact of brain iron accumulation on cognition: A systematic review. *PLoS One*. 2020;**15**(10). e0240697. [PubMed ID: 33057378]. [PubMed Central ID: PMC7561208]. https://doi.org/10.1371/journal.pone.0240697.
38. Ward RJ, Zucca FA, Duyn JH, Crichton RR, Zecca L. The role of iron in brain ageing and neurodegenerative disorders. *Lancet Neurol*. 2014;**13**(10):1045-60. [PubMed ID: 25231526]. [PubMed Central ID: PMC5672917]. https://doi.org/10.1016/S1474-4422(14)70117-6.
39. Onyszchuk G, LeVine SM, Brooks WM, Berman NE. Post-acute pathological changes in the thalamus and internal capsule in aged mice following controlled cortical impact injury: a magnetic resonance imaging, iron histochemical, and glial immunohistochemical study. *Neurosci Lett*. 2009;**452**(2):204-8. [PubMed ID: 19383440]. [PubMed Central ID: PMC2829973]. https://doi.org/10.1016/j.neulet.2009.01.049.
40. Liu HD, Li W, Chen ZR, Zhou ML, Zhuang Z, Zhang DD, et al. Increased expression of ferritin in cerebral cortex after human traumatic brain injury. *Neurol Sci*. 2013;**34**(7):1173-80. [PubMed ID: 23079850]. https://doi.org/10.1007/s10072-012-1214-7.

41. Lin H, Liu H, Tsai P, Hsu F, Lu C, Kao YC, et al. Quantitative susceptibility mapping in mild traumatic brain injury. *Proceedings of the ISMRM*. 2017.
42. Koch KM, Nencka AS, Swearingen B, Bauer A, Meier TB, McCrea M. Acute Post-Concussive Assessments of Brain Tissue Magnetism Using Magnetic Resonance Imaging. *J Neurotrauma*. 2021;**38**(7):848-57. [PubMed ID: 33066712]. [PubMed Central ID: PMC8432603]. https://doi.org/10.1089/neu.2020.7322.
43. Koch KM, Meier TB, Karr R, Nencka AS, Muftuler LT, McCrea M. Quantitative Susceptibility Mapping after Sports-Related Concussion. *AJNR Am J Neuroradiol*. 2018;**39**(7):1215-21. [PubMed ID: 29880474]. [PubMed Central ID: PMC6055518]. https://doi.org/10.3174/ajnr.A5692.
44. Gong NJ, Kuzminski S, Clark M, Fraser M, Sundman M, Guskiewicz K, et al. Microstructural alterations of cortical and deep gray matter over a season of high school football revealed by diffusion kurtosis imaging. *Neurobiol Dis*. 2018;**119**:79-87. [PubMed ID: 30048802]. https://doi.org/10.1016/j.nbd.2018.07.020.